An MRI-based leg model used to simulate biomechanical phenomena during cuff algometry

a finite element study

Manafi-Khanian, Bahram; Arendt-Nielsen, Lars; Graven-Nielsen, Thomas

Published in:
Medical & Biological Engineering & Computing

DOI (link to publication from Publisher):
10.1007/s11517-015-1291-x

Publication date:
2016

Document Version
Accepted author manuscript, peer reviewed version

A MRI BASED LEG MODEL USED TO SIMULATE BIOMECHANICAL PHENOMENA DURING CUFF ALGOMETRY: A FINITE ELEMENT STUDY

Bahram Manafi Khanian, Lars Arendt-Nielsen, Thomas Graven-Nielsen*

Laboratory for Musculoskeletal Pain and Motor Control, Center for Sensory-Motor Interaction (SMI), Department of Health Science and Technology, Faculty of Medicine, Aalborg University, Denmark

Original paper for: Medical & Biological Engineering & Computing

Running head: *Cuff algometry and structural mechanical properties in tissue*

***Corresponding author:**
Thomas Graven-Nielsen, Professor, DMSc, PhD
Laboratory for Musculoskeletal Pain and Motor Control
Center for Sensory-Motor Interaction (SMI)
Department of Health Science and Technology
Faculty of Medicine
Aalborg University
Fredrik Bajers Vej 7D-3
DK-9220 Aalborg E
Denmark
Fax No.: +45 9815 4008
Phone: +45 9940 9832
E-mail: tgn@hst.aau.dk

Total number of words of the manuscript: 6073

Number of words of the abstract: 200

Number of figures: 6

Number of tables: 1

Abstract

Cuff pressure stimulation is applicable for assessing deep-tissue pain sensitivity by exciting a variety of deep-tissue nociceptors. In this study the relative transfer of biomechanical stresses and strains from the cuff via the skin to the muscle and the somatic tissue layers around bones were investigated. Cuff pressure was applied on the lower leg at three different stimulation intensities (mild pressure to pain). Three-dimensional finite element models including bones and three different layers of deep-tissues were developed based on magnetic resonance images (MRI). The skin indentation maps at mild pressure, pain threshold, and intense painful stimulations were extracted from MRI and applied to the model. The mean stress under the cuff position around tibia was 4.6, 4.9 and around fibula 14.8, 16.4 times greater than mean stress of muscle surface in the same section at pain threshold and intense painful stimulations, respectively. At the same stimulation intensities the mean strains around tibia were 36.4%, 42.3% and around fibula 32.9%, 35.0%, respectively of mean strain on the muscle surface. Assuming strain as the ideal stimulus for nociceptors the results suggest that cuff algometry is less capable to challenge the nociceptors of tissues around bones as compared to more superficially located muscles.

Keywords: Cuff algometry, Tissue strain, Tissue stress, Finite-element modelling

INTRODUCTION

Bone-associated pain is severe and adequate treatment remains a challenge [6] where bone metastases are a particular clinical pain management problem. The pathogenesis of bone-related pain is not completely understood; however, the periosteum is innervated by unmyelinated nociceptive afferent which are sensitive to high intensity mechanical stimulation [16,18]. Using several histochemical and imaging techniques, it has been shown that the sensory fibers innervating the periosteum are distinctively organized in a unique net-like meshwork to detect mechanical distortion of the periosteum and underlying mineralized bone [27].

It has been demonstrated that mechanical stimulation and infusion of hypertonic saline into the region of the periosteal tissue at the tibia bone caused pain [17,24]. Direct mechanical stimulation of the periosteum elicited an immediate sharp pain which possessed a significantly lower threshold compared to the stimulation of the ligaments, fibrous capsule of the joints, tendons, fascia, and muscle [27]. Also, chemical stimulation applied around the bone is more painful than when applied to the muscle or subcutaneous adipose layer [15]. These findings suggest the pivotal role of the periosteal layer compared to other tissues in the generation of bone pain. Mechanical stimulations with different probe-size have also been utilized to evoke pain from deep tissues [1,28,33]. The applied pressure is transmitted through the superficial tissues to the deep structures and exciting the deep-tissue nociceptors initiating the pain sensation [14]. The single-point pressure algometry stimulate a localized area around the contact point [10] whereas the computer-controlled cuff algometry stimulates a larger volume of deep somatic tissues and is less influenced by local pain sensitivity variations [13]. Cuff algometry consists of a pneumatically controlled tourniquet cuff by which e.g. pain thresholds, stimulus-response functions, spatial and temporal summation of pain can be assessed [29].

There is limited information about the mechanical influence of pressure algometry on bony structures. The relationships between pressure-induced muscle pain and biomechanical stress and strain generated in skin, subcutaneous adipose, and muscle tissue of the lower leg while stimulation by the single-point pressure algometry on muscle sites have been investigated [8,10,11]. The results suggests that pressure-induced muscle pain is mainly related to strain instead of stress and most efficiently induced by larger rounded probes, whereas small flat probes were less capable to activate the nociceptors of muscle tissue [10]. A finite element (FE) model has been developed to describe the stress and strain distribution in skin, subcutis, and periosteum when the point-pressure stimulation was applied on the tibia bone site with different probe sizes

[9]. It was demonstrated that the mechanical stress of periosteal tissue during the stimulation by the large probe has higher value compared to the small probe. The small diameter probe caused a larger area of the periosteal tissue being strained more intensively compared with the larger diameter probe and hence the small probe was more adequate to evoke bone associated pain [9]. However, no studies have so far attempted to quantify how the mechanical pressure is propagated to the surface of bony structures during the cuff stimulations used for cuff algometry. Cuff algometry has been used for clinical profiling of patients with musculoskeletal pain conditions [21] and thus it is important knowing which tissues are particularly challenged by this methodology. In line, there is a need to compare the influence of cuff algometry on the tissues at the proximity of bony structures and muscle tissues away from the hard tissues. The outcomes would be helpful to contrast the efficiency of cuff algometry for assessment of bone-associated pain compared with the standard single-point algometry.

The aims of this study were to develop a computational finite element model of the lower leg based on magnetic resonance imaging (MRI) data to (1) evaluate stress and strain distribution on the surface of bony structures during cuff compression, (2) relate the pain intensity to the pattern of biomechanical stress and strain distribution on the tissues around bones, and (3) evaluate the capability of cuff algometry for stimulation of tissue around bones compared with more superficially located muscle structures.

MATERIALS AND METHODS

Cuff pressure algometry

Pressure stimulation was applied by a computer-controlled cuff-algometer (Nocitech Aps. and Aalborg University, Denmark) inflated around the lower leg of one healthy subject. The subject did not take any medication during 24 hours prior to the study and did not suffer from acute or chronic pain conditions. The study was conducted in accordance with the Declaration of Helsinki and the human experimental data was a part of a larger study approved by the local ethics committee (N-20130029). Pain detection thresholds (PDT) and pain tolerance threshold (PTT) were recorded using the cuff algometry system. The system consists of a 6-cm wide tourniquet cuff (VBM, Germany) which was wrapped around the right lower leg at the level of the heads of the gastrocnemius muscle. The pressure was increased by 1 kPa/s. The participant described his experience regarding the source of pain and rated the pain intensity continuously during the pressure stimulation on an electronic Visual Analogue Scale (VAS) where zero indicated no pain value and 10 cm the maximal pain intensity. The experiment for detecting the PDT and PTT values was repeated three times with a 2 min interval in-between and the mean of pressure values were used to define three different pressure stimulation intensities: (1) mild stimulation (stimulation with 50% of the PDT), (2) pain detection threshold stimulation (stimulation with the PDT intensity), and (3) intense painful stimulation (5 cm on the VAS).

MRI acquisition

Four magnetic resonance images (MRI) series including the condition without pressure and three different stimulated predefined conditions were performed one day after the assessment of PDT and PTT on the right lower leg of the subject using a 3T MRI scanner (Signa Optima 750, GE Healthcare, Milwaukee, WI, USA). The imaging protocol was based on a matrix of 512×512 pixels, 17 slices for each stimulation condition, 3 mm slice thickness, echo time (TE: 13.664 ms) and repetition time (TR: 660 ms) providing a clear anatomical delineation. The total scanning time was 25 min for all four conditions. The scan encompassed the 6 cm cuff width plus an additional 4.5 cm proximal and distal to the cuff, covering 15 cm of the limb in total.

Indentation map

In order to calculate the nodal displacements of the external surface of the model, a manual segmentation was performed by MATLAB (Mathworks, USA) on total of 68 MRI slices. Ninety nodes were selected on the outline boundary of the limb in each slice. The selected points were connected together making a contour. This contour was unwrapped along the horizontal axis and a curve was generated for each slice indicating the outline boundary as a function of phase angle (θ). This process was implemented on all MRI slices. For each of 17 slices by subtraction of the curves at stimulated conditions from non-stimulated condition the indentation signals were extracted as a function of phase angle. An interpolation function was performed on the indentation curves along the longitudinal axis of the model. Finally the coordination of interpolated data was converted to the Cartesian system for using as a data set while applying the prescribed displacements to the finite element model.

Finite element simulation

The geometry of the model was based on 17 transverse MRI slices at un-deformed condition. Four different anatomical tissues including skin, subcutaneous adipose, muscle and bones were simulated in the finite element model (Fig. 1). 3D image data visualization and volumetric reconstruction (Fig. 1a) of each anatomical structure from MRI slices were performed by Simpleware software (Exeter, UK). The finely detailed three-dimensional mesh was created within the same program based on 853,711 tetrahedral elements and 624,836 degrees of freedom (Fig. 1b). The meshed model was exported to the finite element solver (COMSOL 4.3b Multiphysics, Sweden) software for defining the boundary conditions and material parameters.

All nodes of the soft tissues were left free while the nodes of the bones were only fixed constraint in z-direction; i.e. the bones were left free to have displacement in x and y directions. The bones were assumed to be linear elastic solids with 7300 MPa as Young's modulus and 0.3 as Poisson's ratio [3]. The mechanical behavior of the skin, subcutaneous adipose, and muscle tissue were assumed to be non-linear, isotropic and hyperelastic with the following strain energy density function (W_s) as nearly incompressible version of Neo-Hookean material [7,10,25].

$$W_s = \frac{1}{2}\mu(\bar{I}_1 - 3) + \frac{1}{2}\kappa(J-1)^2$$

Where $\bar{I}_1 = Tr(\bar{F}^T.\bar{F})$ is the first invariant of the isochoric-elastic right Cauchy-Green deformation tensor, $J = \det(F)$ the elastic volume ratio, F the deformation gradient tensor, $\bar{F} = J^{-1/3}.F$ the isochoric component of deformation gradient tensor, and Tr the trace of a matrix. The bulk moduli (κ) and shear moduli (μ) of different soft tissues were adapted from a previous study [34] whereas the material parameters of the skin were reduced by 90 % to prevent the convergence problem [10] which did not have any effect on the stress and strain analysis of other structures. The material constants used in the finite element model were 3000 kPa, 36 kPa, and 116 kPa as bulk modulus and 200 kPa, 1 kPa, and 7.44 kPa as shear modulus for the skin, subcutaneous adipose, and muscle tissue, respectively. The data sets of indentations in three conditions of stimulation were imported in COMSOL and applied incrementally with 0.5 mm step to the external surface of the model. When the intensity of prescribed displacements reached to the final values, the running was stopped.

Stress and strain extraction

Two different surfaces were defined around the bones representing the periosteum of hard tissues with 14,660 mm^2 and 5,167 mm^2 area for the tibia and fibula surfaces respectively. Also, the external surface of the whole muscle tissue with 44,760 mm^2 area was selected as another database. This surface was defined as the interface between the entire tissues of different muscle groups as a unit compartment and the subcutaneous adipose layer. The muscle surface did not include the interface zone in the anterior site of the tibia bone which is not covered by the muscle tissue and is directly subjected to the subcutaneous adipose layer. The patterns of the stress and strain distribution were extracted from finite element simulations at indentations equivalent to the mild, painful and intense painful stimulations. Moreover, the mean and peak values of stress and strain were extracted from the model in correspondence with three different parts of the tibia, fibula and muscle surface including proximal, distal (outside the cuff stimulation area), and cuff position (inside the cuff stimulation area).

RESULTS

Tissue indentation by cuff stimulation

Based on PDT and PTT data, the 9.7±1.4 kPa, 19.4±2.9 kPa, and 30.2±3.8 kPa were used for provocation of mild pressure sensation, pain threshold, and intense painful sensation, respectively. Table 1 shows the absolute indentation value and the location of points which has the greatest indentation at three different stimulation intensities. The 3D map representation of indentations in cylindrical coordinate system extracted from MRI slices and applied to the finite element model is indicated in Fig. 2. A uniform pattern of indentation was not observable along the longitudinal axis (z) of the model and also phase angle (θ) however the indentation values reached the highest magnitude in the longitudinal areas covered by the cuff from z=45 to 105 mm in all three conditions. Interestingly, all the indentations were not compressive in all circumferential areas of the limb. The negative indentations toward the outside of the model happened around the tibia bone site (θ = 81 to 158 deg) while the positive indentation toward the center of the model was observed in other circumferential areas.

Surface stress during cuff pressure stimulations

The three-dimensional finite element simulations showed that the Von-Mises stress on muscle surface (Fig. 3a,b,c), tibia (Fig. 3e,f,g), and fibula (Fig. 3i,j,k) surfaces were increased from the mild to intense painful stimulations. On muscle surface the stress is mainly focused in the cuff position region. The areas with stress concentration were not located in the same z-value for the tibia and fibula surface. The figures depict that the greatest value of stress was in correspondence with the lower parts of the cuff position area for the tibia surface. However, a similar pattern of stress concentration was not observable for the fibula surface meaning the stress was more distributed and not concentrated in a specific point.

For the muscle and bone surfaces located under the cuff position demonstrated the highest value of mean Von-Mises stress (Fig. 4). At mild stimulation the mean Von-Mises stress of muscle surface was 0.61 kPa in the cuff position area while this value was increased by a factor 2.04 in the painful condition. The increasing factor from the mild to intense painful condition was 2.40. At all three stimulation intensities, the mean values of Von-Mises stress on muscle surface in the proximal and distal parts outside the cuff position reduced to 41-49% of mean stress in the cuff area. The mean Von-Mises stress value at mild pressure

condition was 1.35, 2.87, and 1.79 kPa for the proximal, cuff position, and distal part of tibia surface, respectively. These values were increased by factors 2.03, 1.99, and 1.95 from mild to pain threshold condition. Also, the mean Von-Mises stress in these parts for intense painful stimulation was 2.37, 2.49, and 2.19 times greater than mild pressure stimulation. The same increasing pattern was also observable for the fibula surface during the increasing of the stimulation intensity. The mean Von-Mises stress was 6.11, 9.32, and 5.56 kPa for the proximal, cuff position, and distal parts of the fibula surface, respectively. The factor of increase was around 2 for all of these parts from mild to pain threshold condition and 2.54, 2.59, and 2.64 from mild to the highest intensity of stimulation.

Interestingly, the tibia and fibula surfaces demonstrated greater values of mean Von-Mises stress in all three parts compared to the muscle surface. The mean Von-Mises stress in the painful condition in cuff-position section of tibia and fibula surfaces were 4.57 and 14.82 times greater than the same part of the muscle surface, respectively. These factors of increase were 4.87 and 16.53 at the intense painful stimulation.

Surface strain during cuff pressure stimulations

The principal strain had an increasing pattern on the muscle surface (Fig. 5a,b,c), tibia (Fig. 5e,f,g) and fibula (Fig. 5i,j,k) surfaces while increasing the external pressure of stimulation. The strain on muscle surface was not concentrated in a specific area although higher values of mean strain were presented in the part of the muscle surface which was located under the cuff position. On the tibia surface an irregular distribution of strain was visible whereas on the fibula surface the areas with higher values of strain were not located in the cuff position section and mostly distributed outside the cuff area.

The mean principal strain at the muscle surface was generally lower outside the cuff position compared to the cuff area (Fig. 6). In the cuff area the mean principal strain on the muscle surface was 0.048, 0.102, and 0.119 at mild, pain threshold, and intense painful stimulations respectively. The mean values of principal strain in the proximal and distal parts reduced to 60-75% of mean strain in the cuff area at all three stimulation intensities. The mean value of principal strain was almost equal in three different parts of the tibia surface (Fig. 6). The mean principal strain on the tibia surface at mild stimulation was 0.0185, 0.0178, and 0.0191 for proximal, cuff position, and distal parts, respectively, while these values increased to 0.0385, 0.0373, and 0.0390 at pain threshold stimulation, and to 0.0526, 0.0514, and 0.0492 at intense painful

stimulation. The mean strain was not equal in different parts of the fibula surface (Fig. 6). The mean principal strain value of the fibula surface at mild stimulation was 0.0294, 0.0159, and 0.0208 in the proximal, cuff position, and distal parts, respectively. In the painful condition these values increased by factors 2.10, 2.11, 2.06. Also at the intense painful condition they increased by 2.67, 2.62, and 2.68 times greater than mild stimulation.

The muscle surface depicted greatest value of mean strain compared to the bone surface tissues in all three parts of the limb and also at all three stimulation intensities. At painful condition, the mean principal strain of the tibia surface in the cuff area was 36.5% of the mean strain in the same part of the muscle surface and for the fibula surface this value was 32.9%. Moreover, the fibula surface depicted greater values of mean strain in the proximal and distal parts compared with the tibia surface. In the painful condition, the proximal and distal parts of the fibula showed 59.5% and 10.5% increase compared to the same parts of the tibia surface. However, the mean strain of cuff position part of the fibula showed 9.5% decrease compared to the same part of the tibia surface. A similar relationship was observed at mild and intense painful conditions.

DISCUSSION

A three-dimensional finite element model was developed to simulate the stress and strain distribution on musculoskeletal tissues during low and high intensity cuff stimulation of the leg. The structures investigated were the periosteum, covering the surface of bony structures and on the exterior surface of the muscle tissue representing the fascia layers. The simulations showed that cuff algometry is more capable to stimulate the periosteal layers in terms of stress rather than strain compared to the muscle surface (e.g. fascia). However, the muscle surfaces experienced greater strain by the cuff stimulation compared with the periosteal tissues. These points as well as the qualitative experience of the subject describing the muscle pain origination during the cuff stimulation provide new understanding of which structures are activated when cuff algometry is used for profiling patients with musculoskeletal pain.

Three-dimensional map of skin indentation during cuff stimulations

The non-uniform pattern of skin indentation which is applied to the model was predictable because the geometrical shape of the limb is irregular (Fig. 2). Since the cuff pressure is applied to the middle of the lower limb, the profile of skin indentation is not uniform along the z-axis and peaking in the cuff position. Also, inside the cuff position the skin indentation is not flat along the z-axis and demonstrates a bell-shaped profile. Therefore, the highest value of skin indentation is observable at the center of cuff position along the longitudinal axis of the model. Moreover, the indentation profiles along the angle (θ) show that the circumferential areas around the tibia bone site are subjected to the inverse indentation toward the outside of the model; however, the compressive loading is applied to the limb. Due to the inflation of cuff between the leg and bench an upward movement may happen in the limb during MRI. This phenomenon is not observable in the soft tissues because of the compressibility of these layers. The rigidity of bone structures and also the minimal thickness of soft tissues in the anterior site of the tibia, may explain the negative indentation toward the outside of the limb in this region.

Tissue mechanics during pain evoked by cuff pressure stimulations

It has been proposed that pain originating from muscles was diffuse whereas pain originating in fascia, tendon or bone was well localized [23,24]. Periosteal tissues have the highest density of sensory innervation compared to marrow or mineralized bone [26]. Cuff stimulation is normally described as provoking dull and

aching pain [4] whereas deformation of the periosteum generates an intense, sharp, and stabbing pain in quality [31]. Infusion of hypertonic saline close to the periosteum was more painful than similar infusions in muscle and subcutis tissue with respect to pain intensity [15]. It has been suggested that bone pain is caused either by stretching of nerve ending in the periosteum or by micro-fractures in the fragile bone [2]. Interestingly, the external surface of the muscle representing the fascial tissue is known to be densely innervated and highly sensitive in human and animal investigations [19,20,22]. It has been demonstrated increased pain in response to hypertonic saline injection directed to fascial/epimysium tissue as compared with muscle injections following eccentric exercise [12]. In addition, the pressure-evoked pain is highly dependent on mechanical excitation of nociceptors [14]. Mechanical excitation can be potentially affected by factors which have influence on the distribution of mechanical loads inside the different tissues. These factors are thickness of subcutaneous adipose [11], portion of the limb tested [30], calf structure [8], site of pressure stimulation [8,9], and geometrical shape of the probe [10] or cuff. It has been suggested that the sensory innervating fibers of the periosteal layer are ideally located to participate in the development of bone related pain [9].

The present study showed the efficacy of cuff pressure for strain stimulation of fascial tissue and stress stimulation of periosteal layer. The muscle surface demonstrated the highest value of mean strain and lowest value of mean stress compared to the periosteal layers. High local stress on the periosteal layer of hard tissues is supported by the theory of intensive mechanical stress field around the geometric discontinuities. The fibula is the slenderest of the long bones and in present model its area was 35% of the area of the tibia. The higher value of stress on the surface of fibula compared to the tibia is related to the definition of mechanical stress which is a criterion representing the average force per unit area and obviously has an inverse relationship with the total area of the surface. The lower value of mean strain on bone surfaces was also expected because of the proximity of the periosteal layers to the hard tissues.

A previous study about the finite element simulation of single-point pressure algometry indicated that the small probe caused a larger area of the periosteal tissue being strained compared to the larger probe [9]. Large probes mainly excite nociceptors of the muscle tissue whereas smaller diameter probes seem to be more efficient to stimulate nociceptors in the periosteal layers [9]. In present study, the lower strain values of

the periosteal layers compared to the muscle surface tissue may confirm that enlarging the area of external pressure stimulation cannot necessarily increase the biomechanical strain in periosteal layers compared to the superficial muscle tissue. On the other hand, it has been suggested that the mechanical sensitivity of deep tissue nociceptors is mostly related to strain instead of stress [10]. Therefore, it can be hypothesized that cuff pressure stimulation may not be an appropriate way for activation of nociceptors in the periosteal tissues whereas this kind of stimulation is more efficient to elicit nociceptors of the muscle tissue.

Widespread effects of cuff pressure stimulations

The stress distribution follows the bone length and peaks under the cuff position because of the compressive load which is directly applied to this part. At all three stimulation intensities, the mean stress of the tibia and fibula surfaces in the areas outside the cuff position showed 47% and 37% decrease on average compared to the cuff position, respectively. A similar pattern is also observable for the profile of stress distribution on the muscle surface in such way that the average of mean stress decrease in distal and proximal parts was 54%. This demonstrates the higher ability of cuff algometry in periosteal tissues compared to the fascia with respects to transferring of the biomechanical stress from the cuff position to the regions which are not directly subjected to the pressure of cuff.

Similarly, at all stimulation conditions the mean strain distribution of the muscle surface peaks in the cuff area and decrease in the distal and proximal parts, averaging about 32%. However, the strain distribution on the tibia and fibula surfaces does not demonstrate the same process. The strain on the tibia surface is almost evenly distributed in three different parts and showed only 3% average increase in the distal and proximal parts compared to the cuff position. Particularly, in tibia periosteum the strain concentration is more visible in the interface zone between the subcutaneous adipose and the bone which is not covered by muscle tissue and contains nociceptive receptors that respond optimally to high pressure intensity [32]. The strain of fibula periosteum is more concentrated on the proximal and distal parts outside the cuff area and showed 57% increase on average compared to the cuff position which may be related to the tilted position of fibula in the leg and greater value of slenderness ratio compared to the tibia resulting in more inclination to instability. Thus, it can be suggested that the widespread influences of cuff algometry in affecting the areas

outside the cuff compression in terms of biomechanical strain is more strong in the periosteal tissues than the superficial muscle tissue.

Modelling limitations

It has been shown that the mechanical parameters of soft tissues are subject-dependent and even vary with locations on a single subject [35]. For example, the elastic properties of the tissues may be changed in relation to age, sex, and possible pathologies [5]. Therefore, one of the limitations of this modelling is associated to the material constants assigned to the finite element model. Moreover, the outcomes of present study were based on a single subject and may be considered as a single case study. Future studies should include more subjects to draw a general conclusion regarding the capability of cuff algometry for excitation of nociceptors of near-bone tissue.

Because of the irregular geometry of the limb and bell-shape of the cuff after the inflation, the pressure distribution is not uniform along the longitudinal axis of the model and also in transverse planes. This point should be considered in future simulations of cuff efficacies using pressure as load boundary conditions. The compliance of various muscles is not equal among different muscle groups [8]. In present study, all different muscle groups and their connective tissues were considered as a unit compartment in the model. Since the main focus of this study was on the relative transfer of stress and strain from the external surface of the muscle to the periosteum, the details of mechanical interaction between the various muscles were of limited interests.

Conclusion

The results suggest that cuff algometry is less capable to challenge the nociceptors of tissues around bones in terms of strain compared to the superficial muscle tissue. This illustrates the mechanical properties of cuff stimulation and especially how it efficiently targets various structures depending on the location of bony structures which are essential information when assessing the pain sensitivity by cuff algometry.

AKNOWELDGMENTS

The study was supported by a Proof of Concept grant from the Ministry of Higher Education and Science, Denmark. EIR and SMI at Aalborg University are acknowledged for providing facilities and funding for the study. Nocitech is a company partly owned by Aalborg University. The authors have no conflict to report.

References

1. Birtane M, Tuna H, Ekuklu G, Demirbağ D, Tuna F, Kokino S (2004) Pressure-induced pain on the tibia: an indicator of low bone mineral density? J Bone Miner Metab 22:456-461

2. Brandt KD. (1999) Osteophytes in osteoarthritis. Clinical aspects. Osteoarthr Cartilage 7:334-335

3. Cheung JT, Zhang M, Leung AK, Fan Y (2005) Three-dimensional finite element analysis of the foot during standing—a material sensitivity study. J Biomech 38:1045-1054

4. Crews JC, Denson DD, Hilgenhurst G, Bridenbaugh PO, Leavitt B, Stuebing RC (1991) Tourniquet pain: the response to the maintenance of tourniquet inflation on the upper extremity of volunteers. Region Anesth Pain M 16:314-317

5. Cua A, Wilhelm K, Maibach H (1990) Elastic properties of human skin: relation to age, sex, and anatomical region. Arch Dermatol Res 282:283-288

6. Delaney A, Fleetwood-Walker SM, Colvin LA, Fallon M (2008) Translational medicine: cancer pain mechanisms and management. Brit J Anaesth 101:87-94

7. Dubuis L, Avril S, Debayle J, Badel P (2012) Identification of the material parameters of soft tissues in the compressed leg. Comput Method Biomec 15:3-11

8. Finocchietti S, Takahashi K, Okada K, Watanabe Y, Graven-Nielsen T, Mizumura K (2013) Deformation and pressure propagation in deep tissue during mechanical painful pressure stimulation. Med Biol Eng Comput 51:113-122

9. Finocchietti S, Andresen T, Arendt-Nielsen L, Graven-Nielsen T (2012) Pain evoked by pressure stimulation on the tibia bone–influence of probe diameter on tissue stress and strain. Eur J Pain 16:534-542

10. Finocchietti S, Nielsen M, Mørch CD, Arendt-Nielsen L, Graven-Nielsen T (2011) Pressure-induced muscle pain and tissue biomechanics: A computational and experimental study. Eur J Pain 15:36-44

11. Finocchietti S, Mørch CD, Arendt-Nielsen L, Graven-Nielsen T (2011) Effects of adipose thickness and muscle hardness on pressure pain sensitivity. Clin J Pain 27:414-424

12. Gibson W, Arendt-Nielsen L, Taguchi T, Mizumura K, Graven-Nielsen T (2009) Increased pain from muscle fascia following eccentric exercise: animal and human findings. Exp Brain Res 194:299-308

13. Graven-Nielsen T, Arendt-Nielsen L (2010) Assessment of mechanisms in localized and widespread musculoskeletal pain. Nat Rev Rheumatol 6:599-606

14. Graven-Nielsen T, Mense S, Arendt-Nielsen L (2004) Painful and non-painful pressure sensations from human skeletal muscle. Exp Brain Res 159:273-283

15. Graven-Nielsen T, Arendt-Nielsen L, Svensson P, Jensen TS (1997) Experimental muscle pain: a quantitative study of local and referred pain in humans following injection of hypertonic saline. J Musculoskelet Pain 5:49-69

16. Grönblad M, Liesi P, Korkala O, Karaharju E, Polak J (1984) Innervation of human bone periosteum by peptidergic nerves. Anat Rec 209:297-299

17. Hockaday JM, Whitty CW (1967) Patterns of referred pain in the normal subject. Brain 90:481-496

18. Honore P, Mantyh PW (2000) Bone cancer pain: from mechanism to model to therapy. Pain Med 1:303-309

19. Itoh K, Okada K, Kawakita K (2004) A proposed experimental model of myofascial trigger points in human muscle after slow eccentric exercise. Acupunct Med 22:2-12; discussion 12-3

20. Itoh K, Kawakita K (2002) Effect of indomethacin on the development of eccentric exercise-induced localized sensitive region in the fascia of the rabbit. Jpn J Physiol 52:173-180

21. Jespersen A, Dreyer L, Kendall S, Graven-Nielsen T, Arendt-Nielsen L, Bliddal H, Danneskiold-Samsoe B (2007) Computerized cuff pressure algometry: a new method to assess deep-tissue hypersensitivity in fibromyalgia. Pain 131:57-62

22. Kawakita K, Miura T, Iwase Y (1991) Deep pain measurement at tender points by pulse algometry with insulated needle electrodes. Pain 44:235-239

23. Kellgren J. (1938) Observations on referred pain arising from muscle. Clin Sci 3:1937-1938

24. Lewis T. (1938) Study of Somatic Pain. The BMJ 1:321-325

25. Linder-Ganz E, Shabshin N, Itzchak Y, Yizhar Z, Siev-Ner I, Gefen A (2008) Strains and stresses in sub-dermal tissues of the buttocks are greater in paraplegics than in healthy during sitting. J Biomech 41:567-580

26. Mach D, Rogers S, Sabino M, Luger N, Schwei M, Pomonis J, Keyser C, Clohisy D, Adams D, O'leary P (2002) Origins of skeletal pain: sensory and sympathetic innervation of the mouse femur. Neuroscience 113:155-166

27. Martin CD, Jimenez-Andrade JM, Ghilardi JR, Mantyh PW (2007) Organization of a unique net-like meshwork of CGRP sensory fibers in the mouse periosteum: implications for the generation and maintenance of bone fracture pain. Neurosci Lett 427:148-152

28. Nie H, Arendt-Nielsen L, Andersen H, Graven-Nielsen T (2005) Temporal summation of pain evoked by mechanical stimulation in deep and superficial tissue. J Pain 6:348-355

29. Polianskis R, Graven-Nielsen T, Arendt-Nielsen L (2002) Spatial and temporal aspects of deep tissue pain assessed by cuff algometry. Pain 100:19-26

30. Rolke R, Campbell K A, Magerl W, Treede R (2005) Deep pain thresholds in the distal limbs of healthy human subjects. Eur J Pain 9:39-48

31. Sabino MA, Ghilardi JR, Jongen JL, Keyser CP, Luger NM, Mach DB, Peters CM, Rogers SD, Schwei MJ, de Felipe C, Mantyh PW (2002) Simultaneous reduction in cancer pain, bone destruction, and tumor growth by selective inhibition of cyclooxygenase-2. Cancer Res 62:7343-7349

32. Sakada S, Taguchi S (1971) Electrophysiological studies on the free-fiber ending units of the cat mandibular periosteum. Bull Tokyo Dent Coll 12:175-197

33. Takahashi K, Taguchi T, Itoh K, Okada K, Kawakita K, Mizumura K (2005) Influence of surface anesthesia on the pressure pain threshold measured with different-sized probes. Somatosens Mot Res 22:299-305

34. Tran H, Charleux F, Rachik M, Ehrlacher A, Ho Ba Tho M (2007) In vivo characterization of the mechanical properties of human skin derived from MRI and indentation techniques. Comput Method Biomec 10:401-407

35. Vannah WM, Childress DS (1996) Indentor tests and finite element modeling of bulk muscular tissue in vivo. J Rehabil Res Dev 33:239-252

FIGURE LEGENDS

Fig. 1 (a) volumetric reconstruction of the limb including different anatomical structures simulated in the FE model. The figure shows the position of cylindrical coordination system installed on the model (b) three-dimensional meshed model from z = 0 the distal side to z = 150 mm the proximal side with tetrahedral elements used in FE solver. The blue area represents the cuff position

Fig. 2 Three-dimensional representation of indentation maps applied to the external surface of the model in cylindrical coordination system after applying a cubic spline interpolation extracted from MRI data in (a) mild (b) painful and (c) intense painful stimulation. The non-existing indentation from approximately angles 150 to 200 deg represents the position of the tibia bone

Fig. 3 Three-dimensional Von-Mises stress fields extracted from FE simulation on the muscle surface at (a) mild (b) painful, and (c) intense painful stimulations, on the tibia surface at (e) mild (f) painful, and (g) intense painful stimulations and on fibula surface at (i) mild (j) painful and (k) intense painful stimulations. Please note that there is approximately a 20 fold difference in the color coding scale between muscle and bone stress results. The stress on muscle surface and tibia surface is more concentrated in the specific cuff region compared to the fibula surface

Fig. 4 Mean Von-Mises stress at mild, painful, and intense painful cuff stimulation (mild, painful, intense painful) evaluated based on different parts of the muscle, tibia and fibula surfaces extracted from FE simulations

Fig. 5 Three-dimensional principal strain fields extracted from FE simulation on the muscle surface at (a) mild (b) painful and (c) intense painful stimulations, on the tibia surface at (e) mild (f) painful and (g) intense painful stimulations and on fibula surface in (i) mild (j) painful and (k) intense painful stimulations. The strain distribution on all surfaces has an irregular distribution while the muscle surface shows the highest value of strain compared to the periosteal layers

Fig. 6 Mean principal strain at mild, painful, and intense painful cuff stimulation (mild, painful, intense painful) evaluated based on different parts of the muscle, tibia and fibula surfaces extracted from FE simulations

Figure 1
Click here to download Figure: Fig 1.tif

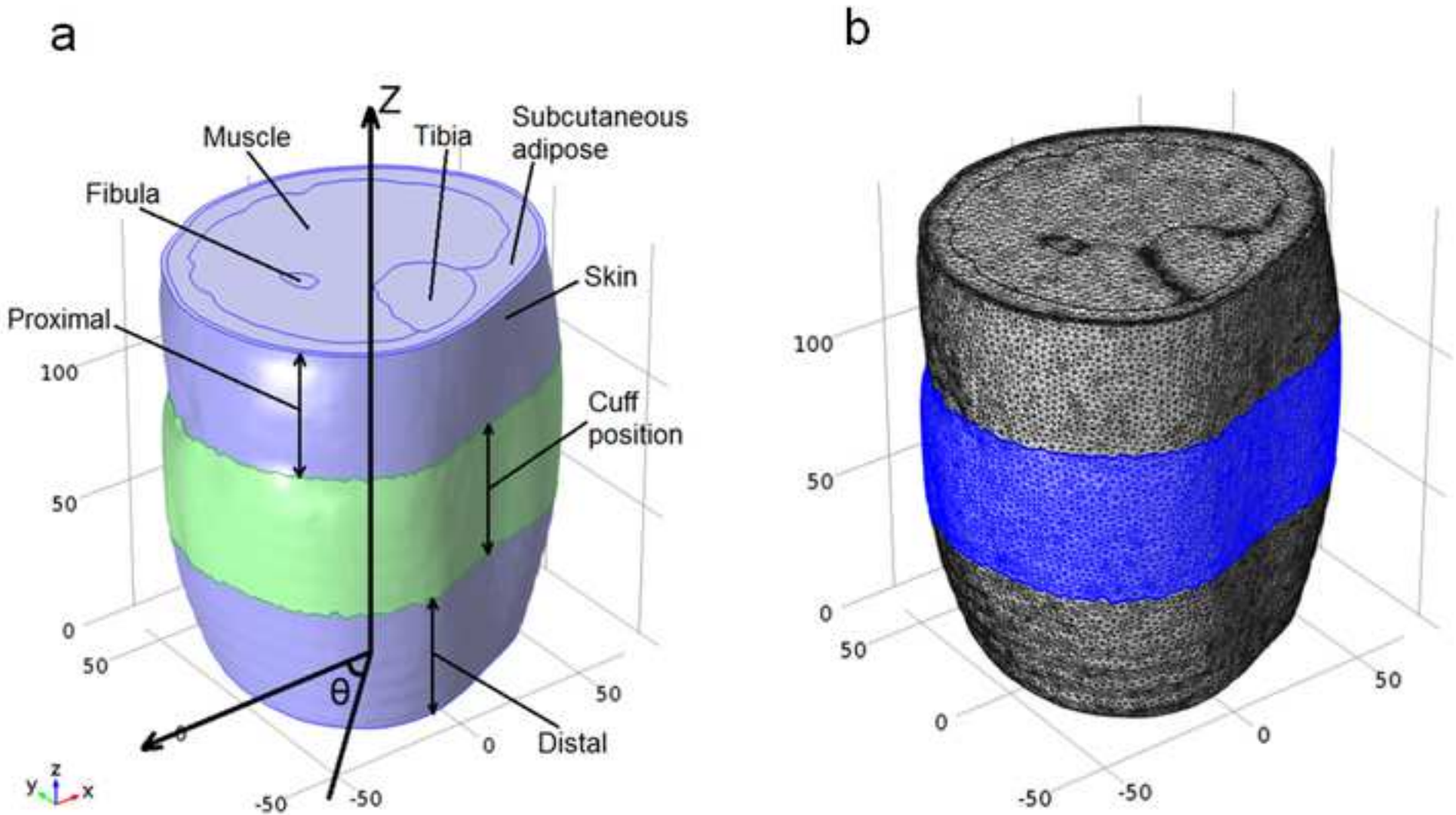

Figure 2
Click here to download Figure: Fig 2.tif

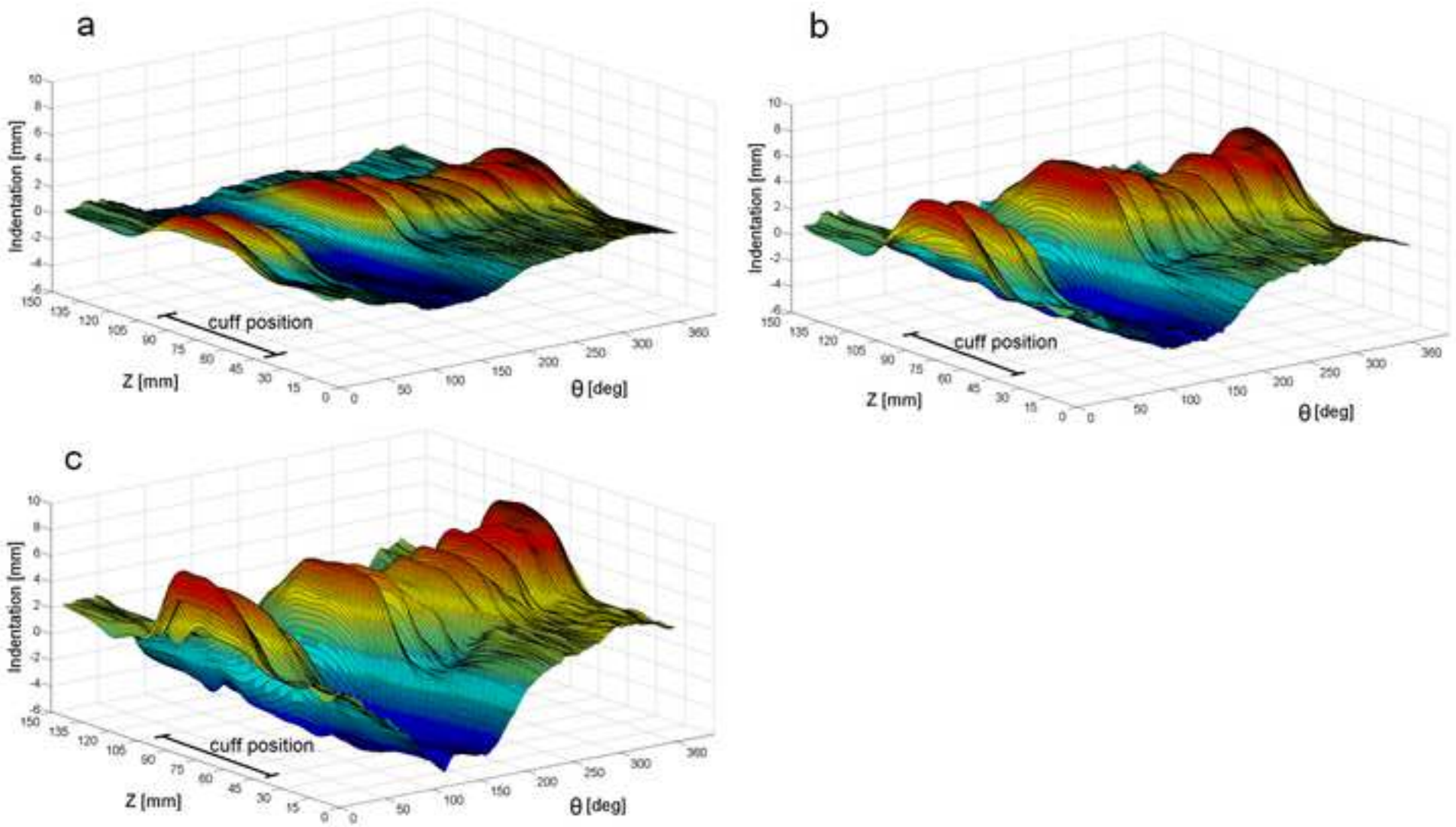

Figure 3
Click here to download Figure: Fig 3.tif

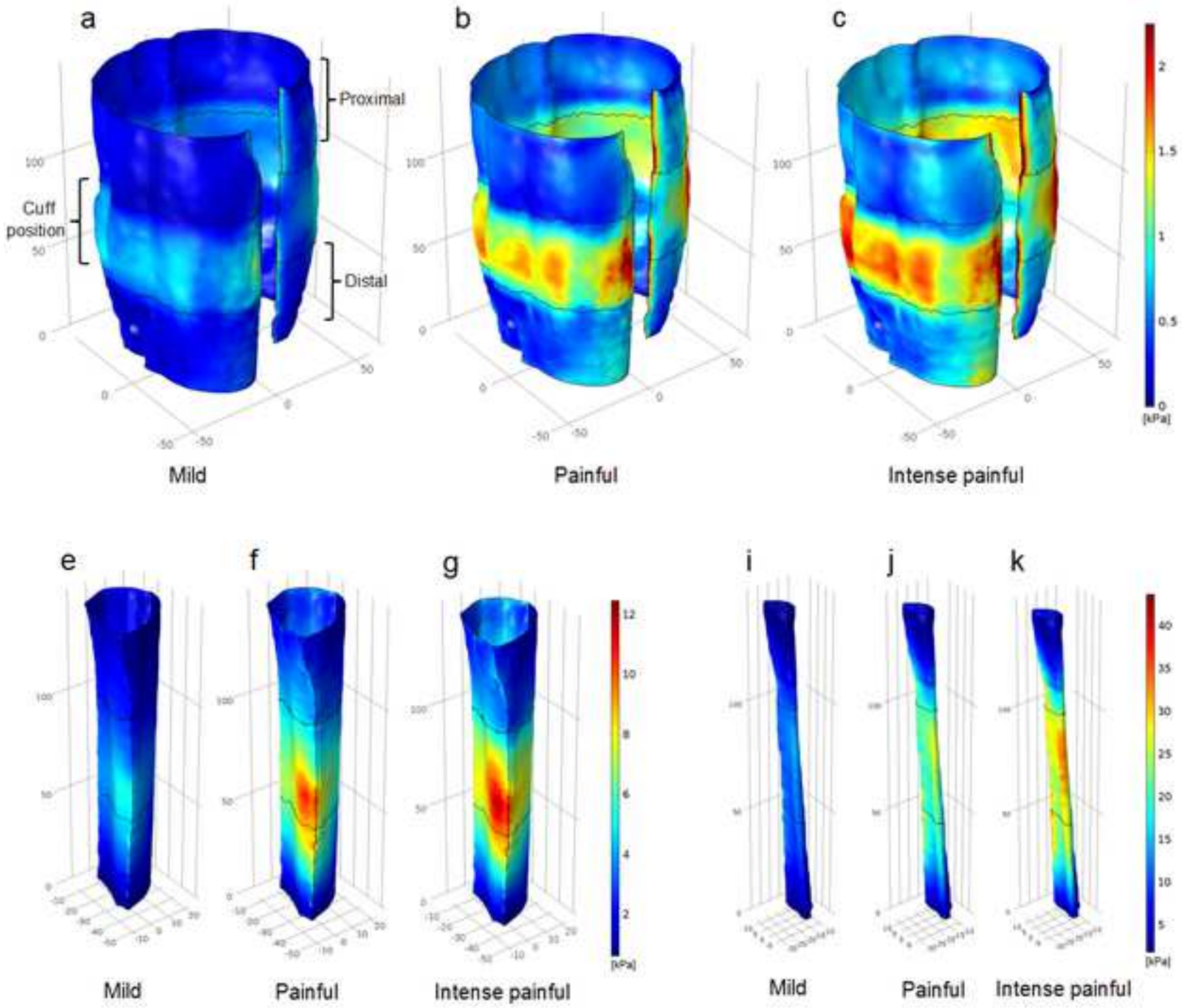

Figure 4
Click here to download Figure: Fig 4.tif

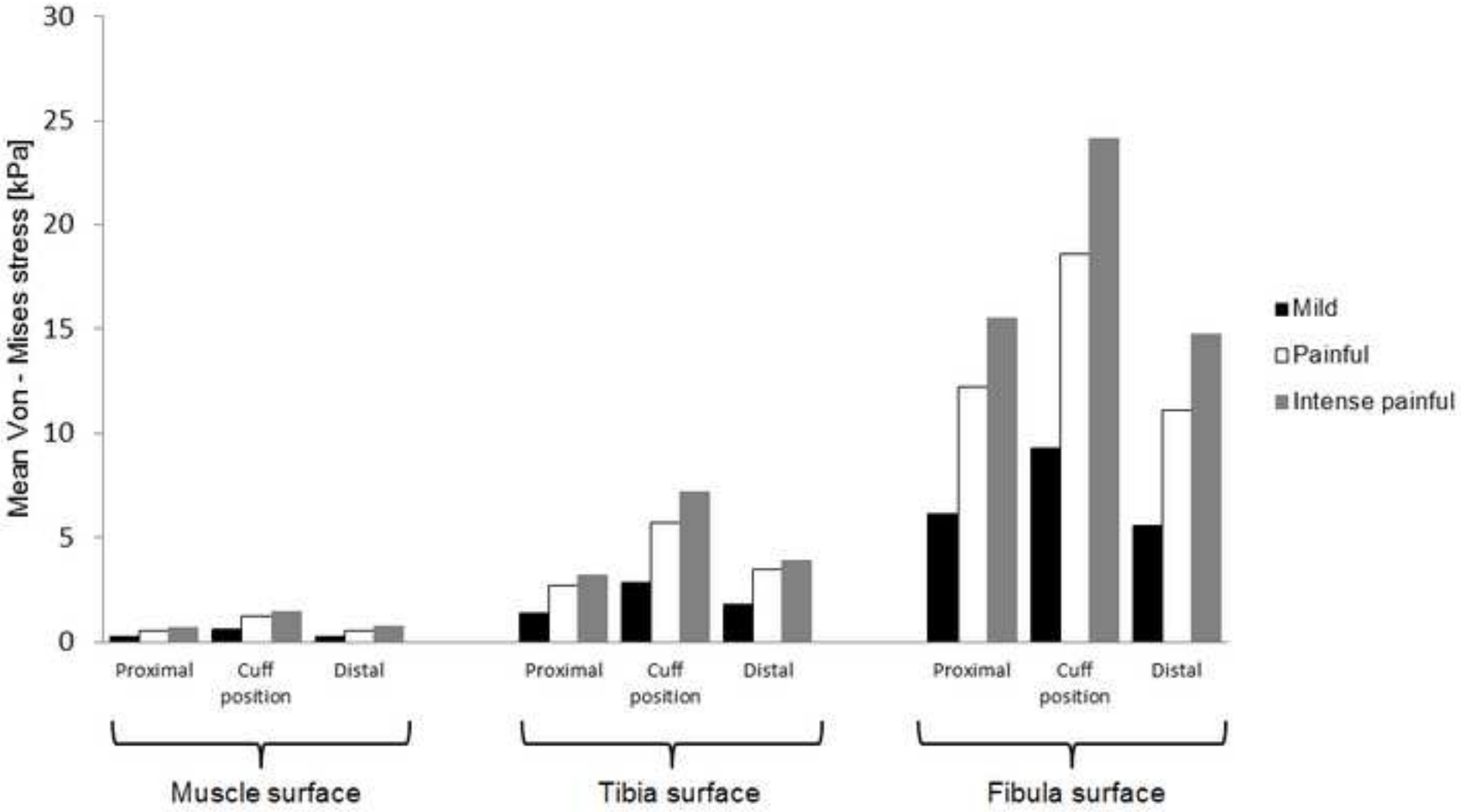

Figure 5

Click here to download Figure: Fig 5.tif

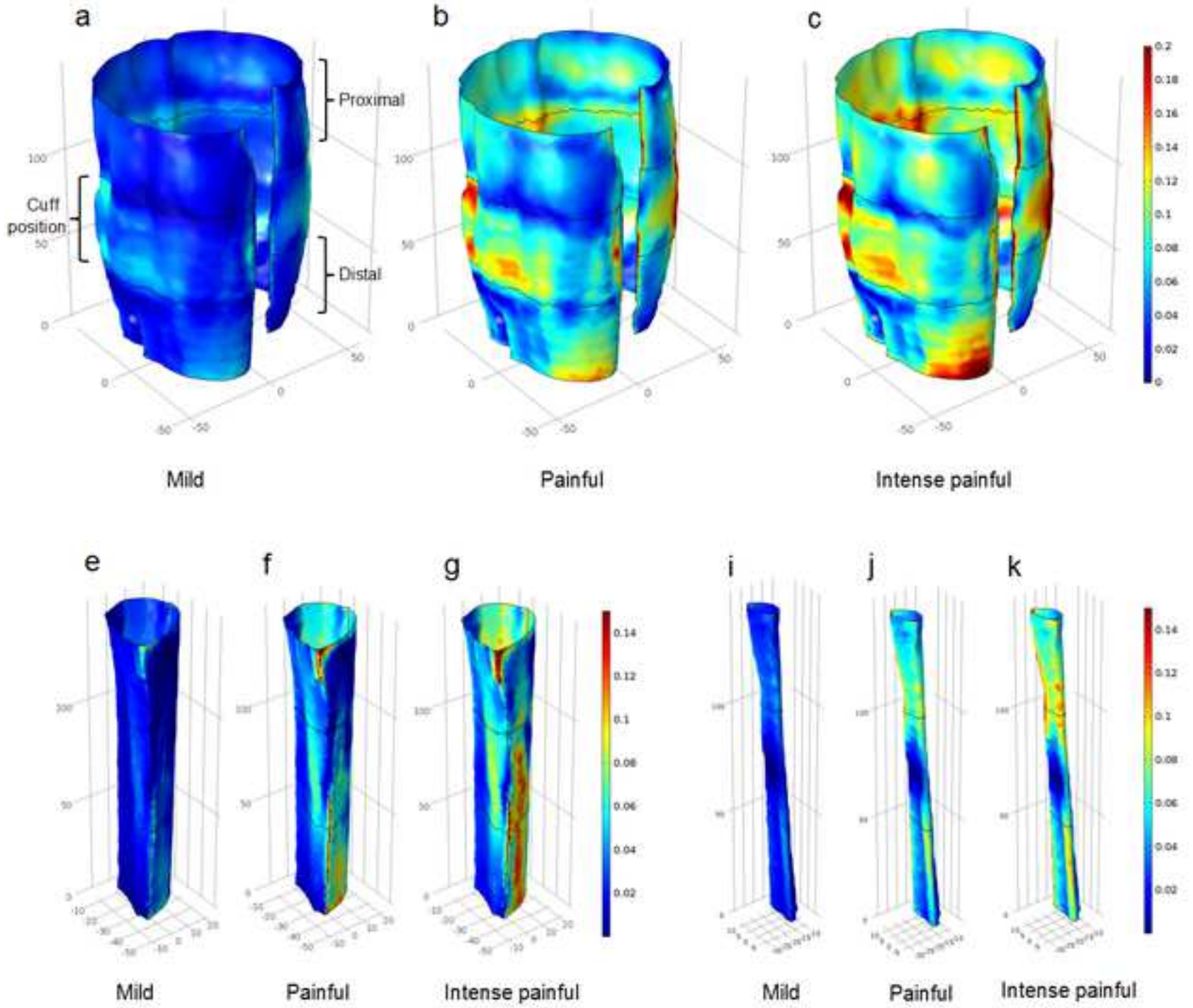

Figure 6
Click here to download Figure: Fig 6.tif

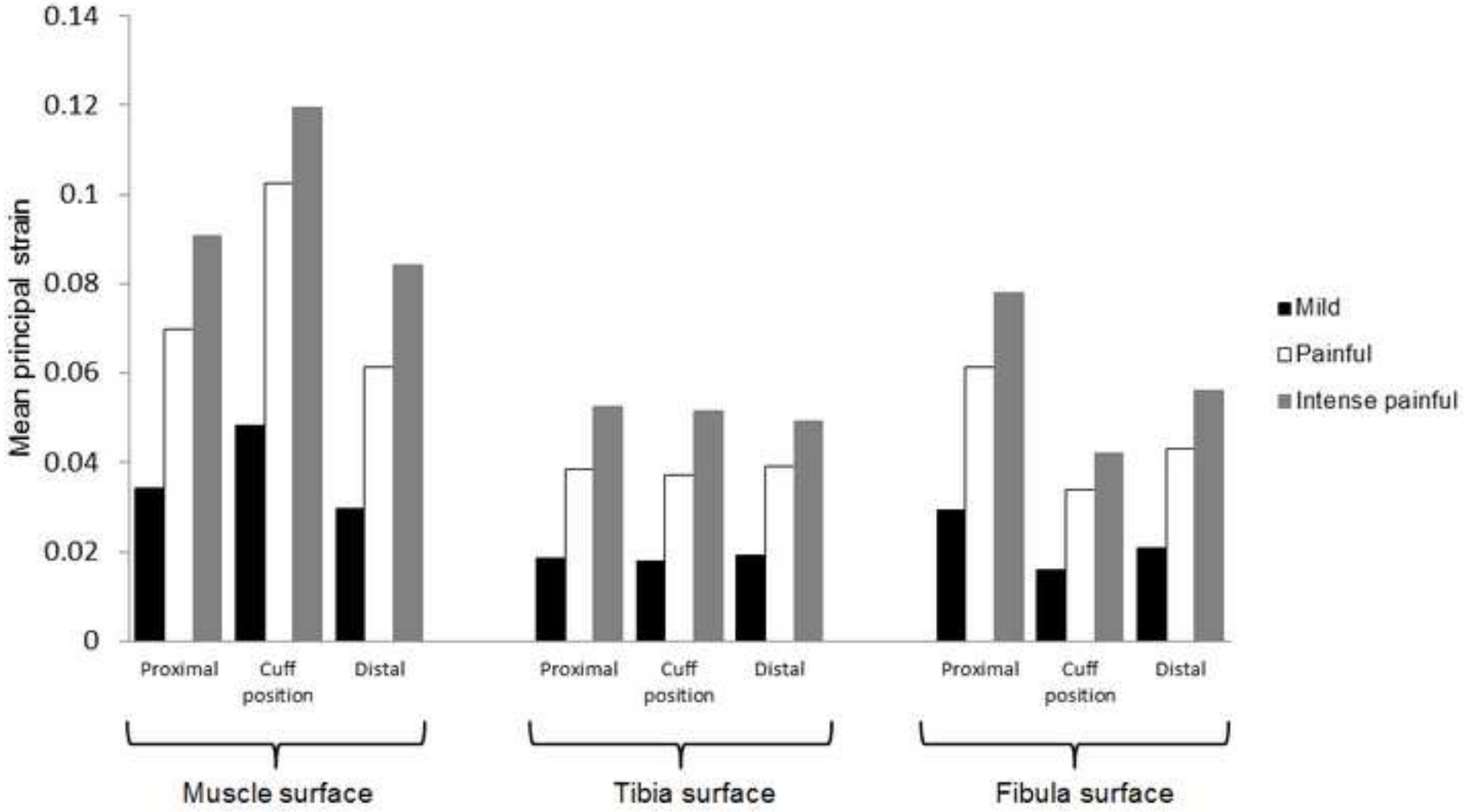

Table 1
Click here to download Table: Table 1.docx

	Mild stimulation		Painful stimulation		Intense painful stimulation	
	Magnitude [mm]	Coordination (θ[deg],z[mm])	Magnitude [mm]	Coordination (θ[deg],z[mm])	Magnitude [mm]	Coordination (θ[deg],z[mm])
Maximum positive indentation	3.4	(348,78)	6.8	(347,77)	8.9	(342,73)
Maximum negative indentation	2.2	(133,55)	4.5	(133,55)	6.0	(134,52)

Table 1 Magnitude and coordination of the points with the highest value of indentation after performing the interpolation on data extracted from MRI slices